33rd Annual International Conference of the IEEE EMBS
Boston, Massachusetts USA, August 30 - September 3, 2011

A quantitative study to design an experimental setup for photoacoustic imaging

Adrien Marion, Jérôme Boutet, Mathieu Debourdeau, Jean-Marc Dinten and Didier Vray

Abstract— **During the last decade, a new modality called photoacoustic imaging has emerged. The increasing interest for this new modality is due to the fact that it combines advantages of ultrasound and optical imaging, *i.e.* the high contrast due to optical absorption and the low acoustic attenuation in biological tissues. It is thus possible to study vascularization because blood has high optical absorption coefficient. Papers in the literature often focus on applications and rarely discuss quantitative parameters. The goal of this paper is to provide quantitative elements to design an acquisition setup. By defining the targeted resolution and penetration depth, it is then possible to evaluate which kind of excitation and reception systems have to be used. First, we recall theoretical background related to photoacoustic effect before to describe the experiments based on a nanosecond laser at 1064 nm and 2.25-5 MHz transducers. Second, we present results about the relation linking fluence laser to signal amplitude and axial and lateral resolutions of our acquisition setup. We verify the linear relation between fluence and amplitude before to estimate axial resolution at 550 μm for a 2.25 MHz ultrasonic transducer. Concerning lateral resolution, we show that a reconstruction technique based on curvilinear acquisition of 30 lines improves it by a factor of 3 compared to a lateral displacement. Future works will include improvement of lateral resolution using probes, like in ultrasound imaging, instead of single-element transducers.**

I. INTRODUCTION

Nowadays, Magnetic Resonance Imaging (MRI), Ultrasound (US) imaging, X-ray Computerized Tomography (CT) and Positron Emission Tomography (PET) are the most used modalities to diagnose pathologies such as cancer. Alternative techniques exist, *e.g.* optical imaging. During the last decade, a new modality called photoacoustic imaging has emerged. It is illustrated by the increase of the number papers related to this topic in SPIE BiOS proceedings, from less than 40 in 2000 to more than 130 in 2010.

Photoacoustic or optoacoustic effect was discovered by G. Bell [1] who experimented production of sounds by periodically illuminating an object with sunlight. This phenomenon was not widely studied untill 1970's due to the lack of adapted light sources. After being studied to estimate gaz concentrations [2], material characterization [3], interest for medicine grew [4].

The increasing interest for this new modality is due to the fact that it combines advantages of ultrasound and optical imaging, *i.e.* the high contrast due to optical absorption and the low acoustic attenuation in biological tissues. Moreover, since photoacoustic imaging depends on optical absoprtion, it is related to physiological processes such as hemoglobin concentration. It is thus possible to study vascularization and for example detect high vascularization due to tumoral angiogenesis [5]. Consequently, photoacoustic imaging provides functional information whereas US imaging can not do it.

Potential applications in biology and medicine are numerous. In the context of small animal imaging, Yang et al. [6] studied cerebral vascularization of a rat and acquire functional information by stimulating rat's whiskers. Another study case is the zebrafish model studied by Razansky et al. [7]. In this paper, the authors are interested in using fluorescent proteins with *in vivo* photoacoustic imaging. Vascular imaging is another field of research well adpated to photoacoustic imaging, which depends essentially on blood optical absorption. As an example, Fronheiser et al. proposed photoacoustic images of arm vasculature [8]. In the same way, Oraevsky et al. were particularly interested in cancerology and presented potential applications for prostate [9] and breast [10].

The research works presented in the literature are often very oriented towards applications and there is not a lot of information about quantitative values. The goal of this paper is thus to provide elements to design an acquisition setup. By defining the targeted resolution and penetration depth, it is then possible to evaluate which kind of excitation and reception systems have to be used. The section II will recall the different parameters implied in the photoacoustic effect and the performed experiments. Then, the results about spatial resolution and strentgh of signal will be detailed before to be discussed in section IV.

II. THEORETICAL BACKGROUND AND EXPERIMENTS

A. Theoretical background

The theoretical background related to photoacoustic effect was widely described by Diebold [11], [12] who studied the generation of photoacoustic signals by a layer, a cylinder and a sphere. Let us recall that the photoacoustic effect is due to a thermal expansion under a temporary light illumination, *e.g.* a laser pulse. The length of the laser pulse has to be smaller than the thermal confinement time given by $\tau_{th} = d_c^2/4D_T$ where d_c is the targeted spatial resolution and D_T the thermal diffusivity. Assuming a value of $0.14\ mm^2.s^{-1}$ and a spatial resolution of $100\ \mu m$, the value of τ_{th} is $1.8\ ms$. The pulse length must also be shorter than the stress confinement time expressed as $\tau_s = d_c/c$ where c is the celerity of acoustic waves, approximately equal to $1540\ m.s^{-1}$ in soft

Thanks to Yannick Guyot for his help during one of our experiments

A. Marion and D. Vray are with Université de Lyon, CREATIS ; CNRS UMR5220 ; Inserm U1044 ; INSA-Lyon ; Université Lyon 1, France. firstname.lastname@creatis.insa-lyon.fr

J. Boutet, M. Debourdeau and J-M. Dinten are with CEA-LETI-DTBS, Grenoble, France firstname.lastname@cea.fr

tissues. With the same spatial resolution, the maximal pulse length is 66 ns. Thus, a nanosecond laser is well adapted to photoacoustic imaging.

Under the previous hypothesis, photoacoustic pressure as a function of space (r) and time (t) is given in Eq. 1 [12]:

$$p(r,t) = \frac{\mu_a \alpha F c^2}{2C_p(r/a)}(1-\widehat{\tau})\widehat{\Theta}_{0,2}(\widehat{\tau}) \quad (1)$$

with

$$\widehat{\tau} = \frac{c}{a}\left(t - \frac{r-a}{c}\right)$$

and

$$\widehat{\Theta}_{u,v}(\widehat{\xi}) = \begin{cases} 1 & \text{if } u < \xi < v \\ 0 & \text{otherwise} \end{cases}$$

In Eq. 1, a is the radius of the spherical absorber, μ_a is the optical absorption (cm^{-1}), α the thermal expansion coefficient (K^{-1}), F the fluence ($J.cm^2$), c the celerity of sound ($m.s^{-1}$) and C_p the specific heat capacity ($J.Kg^{-1}.K^{-1}$). It is straightforward to verify that P is expressed in $kg.m^{-1}.s^{-2}$ or Pa unit.

If we consider quasi constant values of α, c and C_p for soft tissues, then photoacoustic pressures and consequently image contrast will only depend on optical absorption for a given fluence. This is the main interest of photoacoustic imaging since we receive acoustic waves like in ultrasound imaging, but the contrast is related to optical absorption instead of acoustical properties.

From Eq. 1 , we deduce that the length of a photoacoustic signal is given by $\tau = 2a/c$ and starts after $\Delta_T = (D-a)/c$, with D the distance between the center of the absorber and the ultrasound transducer. To illustrate Eq. 1, we simulated a photoacoustic signal generated from a sphere of radius 100 μm, 0.6 mm far from the acoustic transducer in Fig. 1.

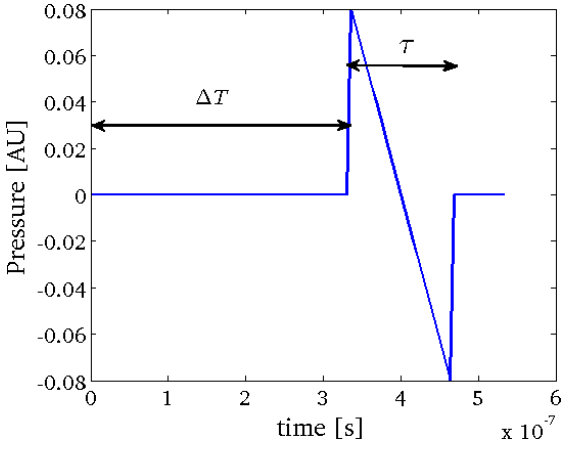

Fig. 1. Shape of a theoretical photoacoustic signal generated by a sphere of radius 100 μm located at 0.6 mm far from the ultrasound transducer

In this figure, we easily find predicted values from Eq. (1), *i.e.* $\Delta_T = 0.333\ \mu s$ and $\tau = 0.133\ \mu s$. This signal is well known as N-shaped signal in photoacoustics. When the absorber is illuminated during a short period, two acoustic waves are generated at the border, one diverging compression wave (first positive peak) and one converging compression wave that becomes a diverging rarefaction wave (second negative peak) after reaching the center. This second wave will then arrive after τ, time necessary to reach the center and go back.

Let us add that the Fourier transform of Eq. 1 is given by:

$$S(\nu) = A\tau e^{-j\pi\nu\tau} e^{-j2\pi\nu\Delta_T} j\left[\frac{sin(\pi\nu\tau)}{(\pi\nu\tau)^2} - \frac{cos(\pi\nu\tau)}{(\pi\nu\tau)}\right] \quad (2)$$

where A is the aplitude of photoacoustic signal.
A limited development tells us that first lobe is located at $x = \pi\nu\tau \approx 2.08$, corresponding to a frequency

$$\nu_{max1} \approx \frac{2.08}{\pi}\frac{1}{\tau} \approx 0.66 \times \frac{1}{\tau}$$

In the case of the N-shaped signal in Fig. 1, the first lobe is located at approximately 5 MHz, that is a conventional frequency used in ultrasound imaging.

B. Experiments

Before to detail experiments, let us now calculate an example value for peak pressure, *e.g.* for blood. With optical absorption $\mu_a = 4.3\ cm^{-1}$ at 1064 nm, thermal expansion coefficient $\alpha = 4.10^{-4}\ K^{-1}$, celerity of sound $c = 1500\ m.s^{-1}$, radius $a = 100\ \mu m$ and fluence $F = 20\ mJ.cm^{-2}$, amplitude is equal to 9.7 kPa.

If we consider acoustic losses in soft tissues close to 0.54 dB/cm/MHz [13], then attenuation at 5 MHz is equal to 2.7 dB/cm. Thus, an ultrasonic signal at a depth of 6 cm is approximately 6.5 weaker when it reaches the transducer. We measured sensitivity of a conventional acoustic transducer (Panametrics, V321) by comparison with an hydrophone (Precision acoustics Ltd, serial number 105) for which we perfectly knew the sensitivity curve as a function of the frequency. We concluded that the minimum detectable pressure at the central frequency was close to 0.6 kPa that is enough to detect the photoacoustic signal.

In the previous section, we mentioned that the length of light pulses had to be smaller than 66 ns. Thus, a lot of research teams chose a laser that deliver nanosecond pulses (between 5 and 20 ns). One team presented a study using a femtosecond laser with a 80 MHz US transducer [14] but this kind of high resolution systems is dedicated to superficial imaging due to the high attenuation factor at these ultrasound frequencies. To image deep biological tissues (several centimeters), conventional systems based on nanosecond pulsed laser and 2-10 MHz transducers are prefered. In this experiment, we used for emission a Q-switched Nd:YAG laser (YHP40 navigator, Spectra physics) emitting pulses of 20 ns at 1064 nm with a pulse repetition frequency (PRF) of 10 Hz. We received ultrasound waves with Panametrics transducers V306 (central frequency 2.25 MHz) or V309 (central frequency 5 MHz) connected to Panametrics Sofranel 40 dB amplifier PR 5052. The amplifier's output was connected to a Lecroy Wave Surfer 44XS oscilloscope to register data. Note here that photoacoustic signals presented in this paper were centered around zero

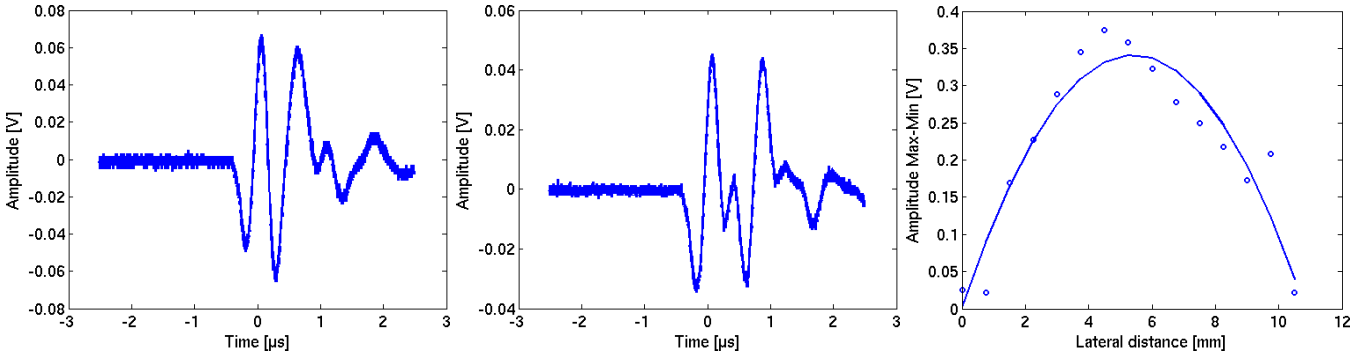

(a) (b) (c)

Fig. 2. Photoacoustic signals received from two wires separated by (a) 400 μm and (b) 700 μm defining axial resolution. (c) Amplitude of photoacoustic signal as a function of the lateral position of transducer defining lateral resolution.

along time axis. In our experiments, we used 600 μm black wires immersed in water.

The first experiment that we conducted consisted in measuring photoacoustic signal amplitude as a function of input energy delivered by laser expressed in mJ/pulse. In the second experiment, we evaluated spatial resolutions along axial (*i.e.* along wave propagation) and lateral axis. For axial resolution, we used two cross 600 μm black wires as we can see in Fig. 3. To evaluate lateral resolution, we acquired successive photoacoustic signals with different lateral positions of transducer. We also performed an image acquisition using 30 lines, separated by 6 degrees, in order to evaluate potential improvement of lateral resolution.

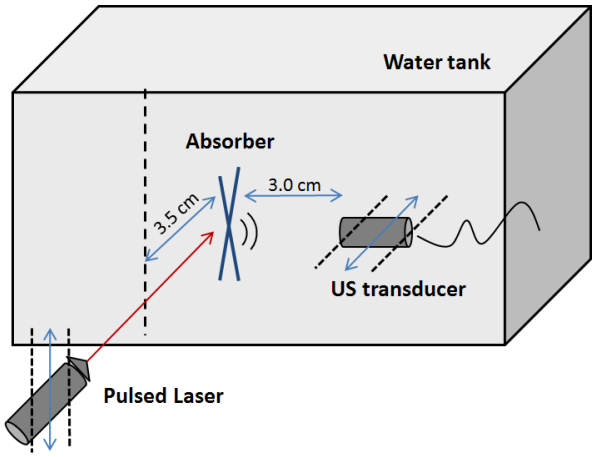

Fig. 3. Synthetic schema of the experiments

III. RESULTS

The first result is presented in Fig. 4 that shows the evolution of the amplitude of photoacoustic signal as a function of the input energy. As we could predict it according to Eq. (1), we see that amplitude is approximately linear as a function of input energy.

In our second experiment, we evaluate axial resolution, *i.e.* the ability to separate the two wires. We see in Fig. 2(a) the resulting photoacoustic signal obtained from two wires

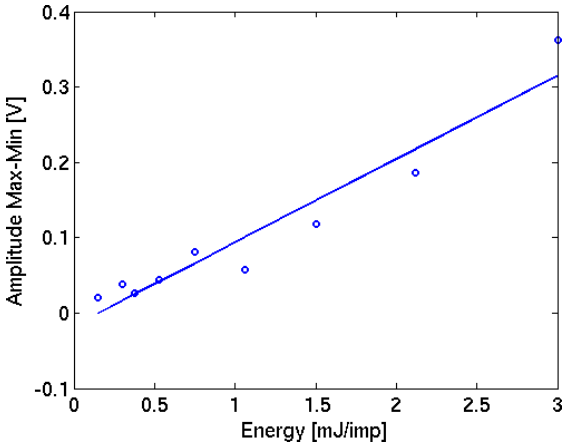

Fig. 4. Amplitude of photoacoustic signal as a function of the input energy

separated by a distance of 400 μm. It is straightforward to see that the axial resolution is higher than 400 μm because contributions of the wires are not separated. Figure 2(b) shows the same signal with a new distance of 700 μm where we see that contributions are separated. Thus we easily conclude that axial resolution is comprised between 400 and 700 μm, approximately 550 μm.

After that, we evaluated lateral resolution illustrated in Fig. 2(c) that is very important. Indeed, it is close to 6 mm if we define it as the full width at half maximum (FWHM). However, we can explain this phenomenon by the use of a large transducer (0.5 inch diameter) not adapted to our objectives. Besides, it is still possible to improve lateral resolution using beamforming techniques. Fig. 5 is a resulting image constructed from the acquisition of 30 lines around 180 degrees. We used a coherent summation technique for the reconstruction. A new lateral profile along horizontal axis shows us a lateral resolution of less than 2 mm, *i.e.* reduced by a factor 3.

IV. DISCUSSION AND CONCLUSION

A. Discussion

Photoacousic imaging is a very promising technique for biomedical applications. Indeed, it opens new potential appli-

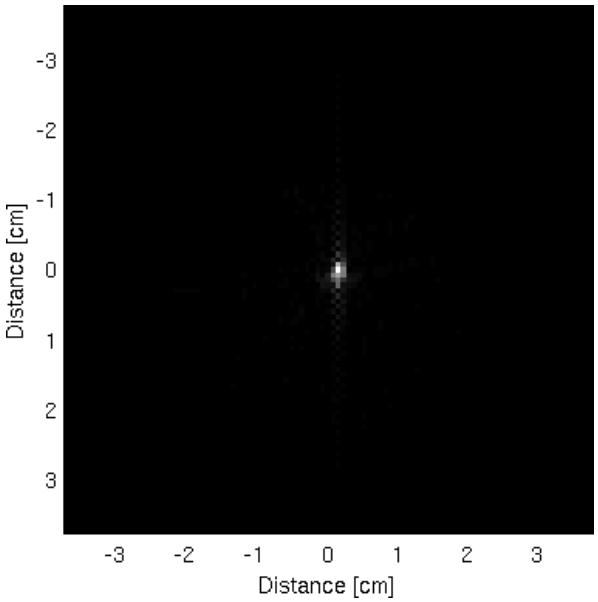

Fig. 5. Photoacoustic image reconstructed from curvilinear acquisition of 30 lines

cations compared to classical ultrasound and optical imaging. In this study, we focused on a quantitative study, rarely mentioned in the literature. In a first time, we recalled important theoretical elements to best understand and quantify photoacoustic phenomenon. In a second time, we verified the linear relation between energy (or fluence) and photoacoustic signal amplitude. Finally, we derived the axial and lateral resolutions of our system.

We showed that lateral resolution was not so good due to the use of a large transducer. A potential solution to improve lateral resolution is to use a needle hydrophone, smaller than a conventional transducer (1 mm). However, the sensitivity becomes highly reduced due to the reduction of the active area. For comparison, the large transducer is sensitive until 0.6 kPa whereas the hydrophone do not detect pressure below 7.5 kPa. It is thus necessary to find a trade-off between sensitivity and lateral resolution.

Concerning axial resolution, the results presented in Fig. 2 were obtained using a 2.25 MHz transducer, giving a wavelength equal to 666 μm with c=1500 $m.s^{-1}$. Thus, the use of a 5 MHz or 7.5 MHz transducer would improve axial resolution by a factor of 2 or 3.

We also showed theoretically that our experimental system (or a similar one) is able to image tissues at a depth higher than 6 cm. Obviously, if sensitivity decreases, then the penetration depth will be reduced in the same way.

B. Conclusion

In this study, we validated an experimental setup adapted to photoacoustic imaging of biological tissues at a depth of several centimeters with axial resolution of hundreds of micrometers. Future works will include improvement of lateral resolution using probes, like in ultrasound imaging, instead of single-element transducers. Thus, beamforming algorithms currently used in ultrasound imaging would be used to obtain a better resolution. A natural development would be fusion of ultrasound and photoacoustic imaging to acquire with a unique system anatomo-functional information.

REFERENCES

[1] A. G. Bell, "On the production of sound by light," *American Journal of Science*, vol. 20, p. 305, 1880.

[2] C. K. N. Patel, E. G. Burkhardt, , and C. A. Lambert, "Spectroscopic measurements of stratospheric nitric oxide and water vapor," *Science*, vol. 184, pp. 1173–1176, 1974.

[3] D. Hutchins and A. C. Tam, "Pulsed photoacoustic materials characterization," *IEEE Transactions on Ultrasonics, Ferroelectrics and Frequency Control*, vol. 33, pp. 429–449, 1986.

[4] A. Rosencwaig, "Potential clinical applications of photoacoustics," *Clinical Chemistry*, vol. 28, pp. 1871–1881, 1982.

[5] H. F. Zhang, K. Maslov, G. Stoica, and L. V. Wang, "Functional photoacoustic microscopy for high-resolution and noninvasive in vivo imaging," *Nature Biotechnology*, vol. 24, pp. 848–851, 2006.

[6] X. Yang, A. Maurudis, J. Gamelin, A. Aguirre, Q. Zhu, and L. V. Wang, "Photoacoustic tomography of small animal brain with a curved array transducer," *Journal of Biomedical Optics*, vol. 14, pp. 054 007–1 – 054 007–5, 2009.

[7] D. Razansky, M. Distel, C. Vinegoni, R. M. N. Perrimon, R. W. Kster, , and V. Ntziachristos, "Multispectral opto-acoustic tomography of deep-seated fluorescent proteins in vivo," *Nature Photonics*, vol. 3, pp. 412–417, 2009.

[8] M. P. Fronheiser, S. A. Ermilov, H. P. Brecht, A. Conjusteau, R. Su, K. Mehta, and A. A. Oraevsky, "Real-time optoacoustic monitoring and three-dimensional mapping of a human arm vasculature," *Journal of Biomedical Optics*, vol. 15, pp. 021 305–1 – 021 305–7, 2010.

[9] M. A. Yaseen, S. A. Ermilov, H. P. Brecht, R. Su, A. Conjusteau, M. Fronheiser, B. A. Bell, M. Motamedi, and A. A. Oraevsky, "Optoacoustic imaging of the prostate: development toward image-guided biopsy," *Journal of Biomedical Optics*, vol. 15, pp. 021 310–1 – 021 310–8, 2010.

[10] S. A. Ermilov, T. Khamapirad, A. Conjusteau, M. H. Leonard, R. Lacewell, T. M. K. Mehta, and A. A. Oraevsky, "Laser optoacoustic imaging system for detection of breast cancer," *Journal of Biomedical Optics*, vol. 14, pp. 024 007–1 – 024 007–14, 2009.

[11] G. J. Diebold, T. Sun, and M. I. Khan, "Photoacoustic monopole radiation in one, two, and three dimensions," *Physical Review Letters*, vol. 67, pp. 3384–3387, 1991.

[12] L. V. Wang, Ed., *Photoacoustic Imaging and Spectroscopy*. CRC Press, 2009, ch. Photoacoustic monopole radiation: waves from objects with symmetry in one, two and three dimensions.

[13] M. O. Culjat, D. Goldenberg, P. Tewari, and R. S. Singh, "A review of tissue substitutes for ultrasound imaging," *Ultrasound in Medicine and Biology*, vol. 36, no. 6, pp. 861–873.

[14] M. E. van Raaij, M. Lee, E. Chrin, B. Stefanovic, , and F. S. Foster, "Femtoseconds photoacoustics: integrated two-photon fluorescence and photoacoustic microscopy," in *Proceedings of SPIE Photonics West, BiOS, Photons plus ultrasound: Imaging and Sensing*, vol. 7564, 2010, pp. 75 642E – 75 642E–6.